Peertechz

Advances and Applications of Bioengineering
OPEN ACCESS JOURNAL

Journal DOI: https://dx.doi.org/10.17352/aabe

Research Article

Activation of the Nrf2 Signaling Pathway by a Ginseng-Salvia-Notoginseng Composite Alleviates Ulcerative Colitis via Restoring Gut Microbiota and Intestinal Barrier

Xinao Lyu[1], Liurong Zhang[1], Jia Si[1], Shasha Dai[1], Huaiyu Su[1], Shuhuan Lyu[1], Lin Chen[1], Jianwei Sun[1], Xiangqun Jin[1]* and Haiyan Li[2]*

[1]Department of Pharmacy, Jilin University, Changchun 130021, China

[2]Department of Pharmacy, Changchun University of Chinese Medicine, Changchun 130021, China

Submitted : 16 February, 2026
Accepted : 19 February, 2026
Published : 20 February, 2026

***Corresponding authors:** Xiangqun Jin, Department of Pharmacy, Jilin University, Changchun 130021, China, E-mail: jinxq@jlu.edu.cn

Haiyan Li, Department of Pharmacy, Changchun University of Chinese Medicine, Changchun 130021, China, E-mail: lihy@ccucm.edu.cn

Keywords: Ulcerative colitis; Nrf2 signaling pathway; Intestinal barrier function; Microbiota dysbiosis; Tight junction proteins; Multi-target therapy

Abstract

Current treatments for ulcerative colitis (UC) often fail to adequately address its multifactorial pathogenesis, involving oxidative stress, barrier dysfunction, and gut microbiota dysbiosis. This study evaluated the therapeutic potential and multi-targeting mechanism of a ginseng, salvia root, and notoginseng oral solution (GSNS) in a DSS-induced mouse colitis model. Based on HPLC-MS/MS technology, 24 major bioactive components were identified. Following the induction of UC with 3.5% dextran sulfate sodium (DSS) in C57BL/6J mice, the animals were treated with GSNS (40, 80, or 160 mg/kg/day) or 5-Amino Salicylic Acid (5-ASA). The therapeutic efficacy was assessed via disease activity, histopathological staining, cytokines, and oxidative stress analysis, and barrier integrity test. Combined data from Western blot, qPCR, immunohistochemistry, electron microscopy, and 16S rRNA sequencing indicate that the therapeutic effect of GSNS against colitis is attributable to its dual role in dampening pro-inflammatory cytokines (TNF-α, IL-6, IL-1β) and potentiating antioxidant defenses via the Nrf2/HO-1 signaling pathway. It also upregulated Occludin expression, repaired tight junctions, and beneficially reshaped the gut microbiota by increasing Prevotellaceae and suppressing *Escherichia-Shigella*. These findings demonstrated that GSNS exerts a multi-target effect against colitis by synergistically enhancing antioxidant defense, repairing the intestinal barrier, and modulating microbial ecology, supporting its potential as a promising natural compound-based candidate for UC treatment.

Introduction

Ulcerative colitis (UC) is a chronic, relapsing inflammatory bowel disease. The core pathology of UC involves disruption to the epithelial barrier, leading to diffuse mucosal injury [1]. Its pathogenesis involves a vicious cycle comprising multiple components, such as oxidative stress, uncontrolled inflammatory responses, and intestinal dysbiosis.

[2-4]. Current therapeutic strategies primarily target specific inflammatory pathways but often fail to address underlying issues such as persistent barrier dysfunction, impaired endogenous antioxidant defences, and gut microbiota dysbiosis [5-7]. This can lead to incomplete remission, high relapse rates, and a suboptimal treatment response in some patients. Consequently, the development of multi-target therapeutic strategies that can intervene in multiple key pathological links of UC simultaneously has become urgent.

Natural products, with their multi-component nature, offer a promising avenue for intervening in this complex pathological network [8]. A classic formulation in traditional Chinese medicine, composed of ginseng (*Panax ginseng*), salvia root (*Salvia miltiorrhiza*), and notoginseng (*Panax notoginseng*),

Citation: Lyu X, Zhang L, Si J, Dai S, Su H, Lyu S, et al. Activation of the Nrf2 Signaling Pathway by a Ginseng-Salvia-Notoginseng Composite Alleviates Ulcerative Colitis via Restoring Gut Microbiota and Intestinal Barrier. Adv Appl of Bioengine. 2026; 2(1): 004-017. Available from: https://dx.doi.org/10.17352/aabe.000003

is renowned for its remarkable efficacy and holds an important position in both theoretical and clinical practice. Key bioactive compounds derived from these herbs, including ginsenosides, salvianolic acids, and notoginsenosides, have demonstrated anti-inflammatory, antioxidant, gut microbiota-modulating, and intestinal barrier-repairing properties [9-11].

While the individual pharmacology of ginseng, salvia root, and notoginseng has been investigated, their combined effects in UC remain unclear [12-15]. Current research has largely focused on single herbs or isolated compounds, lacking a systematic assessment of the overall therapeutic efficacy of the ginseng, salvia root, and notoginseng extract in UC [16-18]. Consequently, the material basis and integrated mechanisms underlying its potential multicomponent synergistic effects are still insufficiently clarified. Moreover, most existing mechanistic investigations are limited to single pathways (e.g., anti-inflammation) and fail to incorporate the interplay between key processes such as Nrf2-mediated antioxidant signaling, intestinal barrier repair, and gut microbiota modulation into a unified framework. A holistic, network-based understanding of the formula's therapeutic actions is thus impeded by the current fragmented approach. At the microbiome level, current evidence is predominantly characterized by compositional descriptions, with a lack of functional validation linking specific microbial shifts, key taxa, or their dynamic interactions to therapeutic outcomes [19]. Therefore, the scientific rationale for using this traditional Chinese medicine (TCM) compound in UC remains incomplete, hindering both systematic formula optimization and the development of precise, mechanism-informed clinical applications.

This study developed the ginseng, salvia root, and notoginseng oral solution (GSNS) and evaluated its therapeutic potential against UC in a DSS-induced mouse model. The chemical profile of GSNS was characterized by LC-MS/MS. Therapeutic efficacy was assessed by monitoring body weight, calculating disease activity indices, measuring colon length, and performing histopathological assessment. To investigate the underlying mechanisms, the expression and localization of inflammatory cytokines, oxidative stress markers, key proteins/genes in the Nrf2 signaling pathway, and tight junction proteins were quantified using enzyme-linked immunosorbent assay (ELISA), Western blot, qPCR, immunohistochemistry (IHC), and immunofluorescence. In parallel, 16S rRNA gene sequencing was performed, combined with diversity analysis, linear discriminant analysis effect size (LEfSe), differential species screening, and correlation network analysis, to systematically elucidate the regulatory effects of GSNS on gut microbiota structure and microbial interaction networks. Collectively, these results demonstrate that GSNS alleviates UC through multi-target mechanisms involving the reduction of oxidative stress, repair of the intestinal barrier, and regulation of gut microbiota ecology.

Materials and methods

Primary chemical reagents

Dextran sulfate sodium (DSS; molecular weight: 40,000 Da, catalogue No. BD123894) was purchased from Bide Pharmatech Co., Ltd. (Beijing, China). Occludin antibody (1:500, BSM-61062R) was purchased from Bioss (Beijing, China). Antibodies against Nrf2/NFE2L2 (66504-1-Ig), HO-1/HMOX1 (66743-1-Ig), GAPDH (66004-1-Ig), and Lamin B1 (66095-1-Ig) were obtained from ProteinTech (Wuhan, China). ELISA kits for interleukin-6 (IL-6), interleukin-10 (IL-10), interleukin-1β (IL-1β), myeloperoxidase (MPO), tumour necrosis factor-α (TNF-α), malondialdehyde (MDA), glutathione (GSH), and superoxide dismutase (SOD) were purchased from FeiYa Biotechnology Co., Ltd. (Nanjing, China) and Multi Sciences (Hangzhou, China), respectively. TRIzol reagent was obtained from Invitrogen (Carlsbad, CA, USA). RIPA lysis buffer (containing PMSF; catalogue No. P0013B), phenylmethylsulfonyl fluoride (PMSF; catalogue No. ST505), and a bicinchoninic acid (BCA) protein assay kit (catalogue No. P0012) were purchased from Beyotime Biotechnology (Shanghai, China). A polyvinylidene fluoride (PVDF) membrane (catalogue No. IPVH00010) was obtained from Millipore (Burlington, MA, USA). The 16S rRNA gene (V4 region) Amplification and Library Preparation Kit (catalogue No. 12933ES96) was purchased from Yeasen Biotechnology Co., Ltd. (Shanghai, China). The following reagents and kits were purchased from Servicebio Biotechnology Co., Ltd. (Wuhan, China): Magnetic Bead-Based Bacterial Genomic DNA Extraction Kit, Universal Tissue Fixative, Optimal Cutting Temperature (OCT) Embedding Medium, Hematoxylin and Eosin (H&E) Staining Kit, RNA Extraction Reagent, SweScript All-in-One RT SuperMix, and 2×Universal Blue SYBR Green qPCR Master Mix. Sequencing was performed on the DNBSEQ-G99 platform by Shenzhen BGI Intelligent Manufacturing Technology Co., Ltd. (Shenzhen, China).

Preparation of ginseng, salvia root, and notoginseng oral liquid

The compound extract GSNS was prepared using a standardized reflux extraction protocol. Briefly, authenticated crude drugs of ginseng, salvia root, and notoginseng were mixed in a 1:1:1 weight ratio. The mixture underwent two rounds of reflux extraction with 50% ethanol solution (10: 1, v/w), each for 3 hours. The combined extracts were filtered, and the filtrate was concentrated under reduced pressure at 40 - 50°C using a rotary evaporator. The resulting concentrated liquid was then lyophilized to a constant weight, yielding the dry extract powder. The extraction yield was calculated accordingly. For in vivo administration, a precise weight of the lyophilized powder was reconstituted in sterile distilled water to the desired concentration. The solution was sterilized by filtration through a 0.22 μm membrane and aliquoted for storage at -20°C.

Chemical profiling of GSNS using UPLC-MS/MS

UPLC-MS/MS analysis was performed on a Dione× UltiMate 3000 system coupled to a Thermo Q-Exactive Plus mass spectrometer to determine the chemical constituents of GSNS, according to a published method [20]. Chromatographic separation utilized an ACQUITY UPLC HSS T3 column (150×2.1 mm, 1.8 μm). The mobile phase consisted of (A) deionised water containing 0.1% formic acid and (B) acetonitrile containing 0.1% formic acid. These were delivered in gradient elution

Citation: Lyu X, Zhang L, Si J, Dai S, Su H, Lyu S, et al. Activation of the Nrf2 Signaling Pathway by a Ginseng-Salvia-Notoginseng Composite Alleviates Ulcerative Colitis via Restoring Gut Microbiota and Intestinal Barrier. Adv Appl of Bioengine. 2026; 2(1): 004-017. Available from: https://dx.doi.org/10.17352/aabe.000003

mode as follows: 0 - 5 min: 5% B; 5 - 95 min: 5% to 95% B (linear gradient); 95 - 100 min: 95% B. Thereafter, the system was returned to the initial conditions (95% A, 5% B) within 0.1 min, after which it was equilibrated for 10 min. A constant flow rate of 0.3 mL/min was maintained throughout the run. Data acquisition and processing were carried out using Xcalibur and TraceFinder 5.1 software (Thermo Fisher Scientific, Waltham, MA, USA).

Animals and handling

Male C57BL/6J mice weighing 20 ± 2 g were obtained from Speifu (Beijing) Biotechnology Co., Ltd. (Changchun, China; licence no. SYXK (Ji) 2021-0003). After a three-day acclimatisation period under controlled conditions (25 ± 2℃, 60 ± 5% relative humidity, 12 h light/dark cycle), the mice were randomly divided into six groups (n = 6). The control group received normal drinking water. The model group received 3.5% (w/v) DSS in drinking water for 7 days. The positive control group received 3.5% DSS water plus 5-ASA (100 mg/kg/day) by oral gavage. Three treatment groups ($GSNS_L$, $GSNS_M$, $GSNS_H$) received 3.5% DSS water plus GSNS at doses of 40, 80, and 160 mg/kg/day, respectively, via oral gavage. Drug administration (5-ASA and GSNS) was performed daily from day 4 to day 10. On day 11, all mice were euthanised. Peripheral blood was collected via orbital bleeding, and colon tissues as well as intestinal contents were immediately harvested for subsequent analysis (see experimental timeline in Figure 2). Animal experiments used six mice per group (n = 6) based on pilot study effect sizes for sufficient statistical power. For molecular analyses (Western blot, qPCR), three randomly selected samples per group (n = 3) served as biological replicates, sufficient to validate in vivo mechanisms. This design follows the Reduction principle of the 3R framework (Replacement, Reduction, Refinement), minimizing animal use while maintaining data reliability [21]. All assays included three technical replicates. All procedures were approved by the Animal Care and Use Committee of the School of Pharmacy, Jilin University (Approval No. 20250121) and conducted in accordance with relevant guidelines.

Mouse body weight, disease activity index, and colon length

Body weights were recorded for all mouse groups each day before treatment; fecal samples were simultaneously evaluated for consistency and signs of bleeding. The disease activity index (DAI) score provides a comprehensive reflection of disease severity in the UC model mice. The calculation formula is: DAI = (Body Weight Loss Score + Fecal Consistency Score + Blood in Feces Score) / 3 [22]. Photograph the colon and measure its length to assess the degree of inflammatory response.

Analysis of serum and colon cytokines and oxidative stress markers

Blood samples were processed by centrifugation at 4,000 rpm for 20 minutes at 4℃ to obtain the serum. Colon samples were homogenised in PBS and centrifuged at 13,000 rpm for 10 minutes to collect the supernatant. Commercial ELISA kits were used to quantify the levels of cytokines (TNF-α, IL-6, IL-10, and IL-1β) in both the serum and the colonic supernatant, and the levels of oxidative stress markers (MPO, MDA, SOD, and GSH) in the colonic supernatant, according to the manufacturers' instructions.

Hematoxylin-eosin staining and immunohistochemical analysis of mouse colon tissue

Histopathological assessment was conducted based on H&E staining. After routine processing (fixation in 4% paraformaldehyde, paraffin embedding, and sectioning), tissue sections were scored for pathological changes using an established criterion [23]. To detect Nrf2 using IHC, the paraffin sections were subjected to antigen retrieval. Subsequently, endogenous peroxidase was quenched with 3% CH_3OH-H_2O_2, and non-specific sites were blocked with 3% bovine serum albumin (BSA). The sections were then incubated with an anti-Nrf2 primary antibody overnight at 4℃ in a humidified chamber, followed by incubation with a horseradish peroxidase (HRP)-conjugated secondary antibody. Signal visualisation was achieved using 3,3'-diaminobenzidine (DAB) as the chromogen, and the development time was monitored under a microscope. Finally, the sections were counterstained with haematoxylin, dehydrated, cleared, and mounted. Protein expression of Nrf2 was quantified using the H-Score method.

The semi-quantitative scoring system evaluates both staining intensity and the proportion of positive cells. The staining intensity was graded on a scale of 0 to 3 (0, negative; 1, weak/pale yellow; 2, moderate/brownish yellow; 3, strong/dark brown). The H-Score was calculated using the formula: H-Score = $\sum$ (pi×i), where 'i ' is the intensity score (0 - 3) and 'pi' is the percentage of cells stained at that intensity [24].

Immunofluorescence staining of tight junction proteins

For the localization of tight junction proteins, processed colon sections (from Section 2.7) were subjected to standard immunofluorescence staining. The sections were incubated overnight at 4°C with primary antibodies against ZO-1 and Occludin. After PBS washes, they were incubated with fluorochrome-conjugated secondary antibodies for 1 h at 37°C and then counterstained with DAPI. High-resolution images were acquired using a Leica TCS STELLARIS 5 confocal microscope to assess protein Distribution.

Ultrastructural analysis of mouse colon via transmission electron microscopy

Following initial fixation in 4% glutaraldehyde, the colon tissues were prepared for transmission electron microscopy (TEM). This involved sectioning, dehydration, embedding, polymerisation, and ultrathin sectioning (4 μm). The sections were then post-stained with uranyl acetate and lead citrate, after which they were observed under a Hitachi HT7700 TEM (Japan).

RNA extraction and real-time fluorescent quantitative PCR analysis

ColonTotal RNA was extracted from colon tissue using TRIzol reagent and precipitated with isopropanol. Total

Citation: Lyu X, Zhang L, Si J, Dai S, Su H, Lyu S, et al. Activation of the Nrf2 Signaling Pathway by a Ginseng-Salvia-Notoginseng Composite Alleviates Ulcerative Colitis via Restoring Gut Microbiota and Intestinal Barrier. Adv Appl of Bioengine. 2026; 2(1): 004-017. Available from: https://dx.doi.org/10.17352/aabe.000003

RNA was first quantified for concentration and purity on a NanoDrop 2000 Spectrophotometer (Thermo Fisher Scientific, USA). Subsequently, 1 µg of RNA was reverse-transcribed into cDNA using the SweScript All-in-One SuperMix for qPCR Kit (Servicebio, China) following the kit protocol. Quantitative PCR was then carried out on a StepOnePlus™ System (Applied Biosystems, USA) with Universal Blue SYBR Green qPCR Master Mix (Servicebio, China). After an initial 30 s step at 95℃, samples underwent 40 cycles of denaturation (95℃, 15 s) and annealing/extension (60℃, 30 s). Specificity was assessed by melting curve analysis. Gene expression was quantified relative to the geometric mean of Ywhaz and Hprt1 using the $2^{-\Delta\Delta Ct}$ method. For miRNA analysis, miR-146a-5p was normalized against U6 as the reference gene. Primer sequences are listed in Table 1.

Protein expression analysis of relevant signaling pathways (Western Blot)

Total protein was extracted from colon tissues with RIPA lysis buffer supplemented with PMSF, and concentrations were quantified using a BCA assay kit. Equal protein aliquots were then separated by SDS-PAGE and electrophoretically transferred onto PVDF membranes. Following blocking, the membranes were probed overnight at 4℃ with primary antibodies against Occludin, Nrf2, HO-1, Lamin B1, and GAPDH. GAPDH and Lamin B1 served as loading controls for cytoplasmic and nuclear proteins, respectively. After washing, the blots were incubated with horseradish peroxidase (HRP)-conjugated secondary antibodies for 1 h at room temperature. Band detection was performed with a JUNYI chemiluminescent imager. Quantitative analysis was carried out by measuring the optical density of each band using Image J software (NIH, Version 1.8).

Microbial community analysis based on the 16S rRNA Gene

The resulting amplicons were purified, pooled in equimolar amounts, and prepared for sequencing library construction. Sequencing was performed on the DNBSEQ-G99 platform (2 × 00 bp paired-end), yielding approximately 50,000 raw reads per sample. Data processing was conducted within the QIIME2 (v202.5) workflow. Processing of the raw 16S rRNA sequencing data involved demultiplexing, quality filtering, merging, and denoising using DADA2, followed by clustering into amplicon sequence variants (ASVs). Taxonomic annotations for the ASVs were derived from the SILVA 138 database.

Subsequent analyses included α-diversity metrics (Chao1, Simpson, Shannon, richness, Pielou, and observed ASVs), a β-diversity analysis via PCoA based on Bray-Curtis and Jaccard distances, an examination of ASV sharing using Venn diagrams, and a profiling of community composition at phylum, genus, and species levels, supplemented by a phylogenetic tree. LEfSe was applied to identify key differential microbial features (LDA score > 3.5), listing the top 30 most significant taxa. Finally, a species abundance-based correlation network was constructed. This integrated analysis provided a systematic characterisation of DSS-induced colitis and the impact of GSNS intervention on the structure of the murine gut microbiota.

Statistical Analysis

Statistical analysis was performed using GraphPad Prism 10.0 (GraphPad Software, USA) and SPSS Statistics 22.0 (lBM, Armonk, NY, USA). All data are presented as mean ± standard error of the mean (SEM) from at least three independent experiments. For comparisons among multiple groups, one-way analysis of variance (ANOVA) followed by Tukey's post-hoc test was conducted using SPSS. Statistical significance was set at $p<0.05$, and significance levels are indicated as follows: $*p < 0.05$, $**p < 0.01$, $***p < 0.001$.

Results

LC-MS/MS-Based Identification of Bioactive Constituents in GSNS

The chemical profile of GSNS was established by LC-MS/MS analysis. A total of 25 major bioactive components were identified by comparing retention times and mass spectra with authenticated reference standards (see the total ion chromatogram in Figure 1). These components included various ginsenosides (e.g. 20(R)-ginsenoside Rg2, ginsenoside Rb1 and Rg1) [25-27], notoginsenosides (e.g. notoginsenosides R1) and Salvianolic acids (e.g., salvianolic acid B) [28,29]. Identification

Table 1: Primer Sequences Used for Gene Expression Analysis by RT-qPCR.

Gene		Primer Sequences (5'to 3')	Fragment Size (bp)	Gene Accession Number
KEAP1	Forward Reverse	GAGATATGAGCCAGAGCGGGA AACTGGTCCTGCCCATCGTAG	270	NM_001110305.1
GCLC	Forward Reverse	CTGTAGATGATAGAACACGGGAGG GAGATGAGCAACGTGCTGTGC	215	NM_010295.2
Srxn1	Forward Reverse	GTACCAATCGCCGTGCTCAT GAGCTTGGCAGGAATGGTCT	222	NM_029688.6
Ywhaz	Forward Reverse	TTGTAGGAGCCCGTAGGTCATC CAGCAACCTCGGCCAAGTAA	249	NM_001253805.1
Hprt1	Forward Reverse	TCATGGACTGATTATGGACAGGACT GCTTTAATGTAATCCAGCAGGTCAG	138	NM_013556.2
miR-146a-5p	Forward	CTCAACTGGTGTCGTGGAGTCGGCAATTCAG TTGAG AACCCATG	66	MIMAT0000158
U6	Reverse Forward Reverse	ACACTCCAGCTGGGTGAGAACTGAATTCCA CTCGCTTCGGCAGCACA AACGCTTCACGAATTTGCGT	94	NR_004394.2

Citation: Lyu X, Zhang L, Si J, Dai S, Su H, Lyu S, et al. Activation of the Nrf2 Signaling Pathway by a Ginseng-Salvia-Notoginseng Composite Alleviates Ulcerative Colitis via Restoring Gut Microbiota and Intestinal Barrier. Adv Appl of Bioengine. 2026; 2(1): 004-017. Available from: https://dx.doi.org/10.17352/aabe.000003

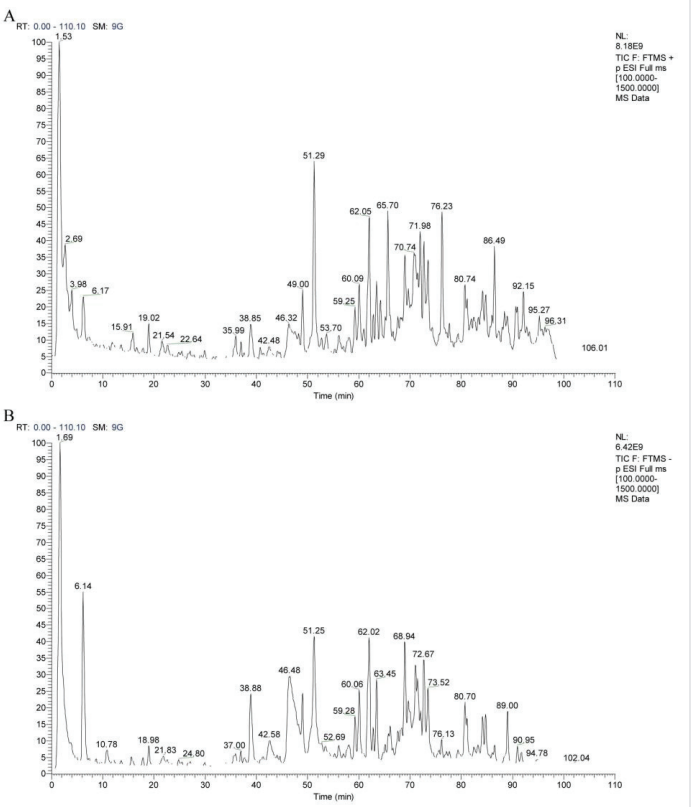

Figure 1: Total ion chromatography (TIC) of the GSNS extract. (A) Profile obtained in positive ion mode. (B) Profile obtained in negative ion mode.

criteria were set at a mass error tolerance of <3 ppm and an identification score of >80 [30]. Detailed data for each compound are summarised in Table 2, thereby elucidating the material basis underlying the pharmacological efficacy of GSNS (Figure 1).

Impact of GSNS on DAI and Associated Metrics

The experimental design and treatment timeline are summarized in Figure 2A. As shown in Figure 2B, gross examination of colon tissues revealed marked shortening and atrophy in the model group compared to the control. Quantitative measurement confirmed this observation, indicating that colon length in the model group was significantly reduced ($p < 0.001$, Figure 2C). Regarding dynamic disease progression, control mice exhibited steady weight gain throughout the experiment, while model group mice showed progressive weight loss from day 4 onward (Figure 2D). Concordantly, the DAI remained low in controls but rose sharply in the model group (Figure 2E). Intervention with GSNS dose-dependently alleviated DSS-induced weight loss ($P < 0.05$, Figure 2D) and significantly reduced DAI scores in the high-dose group ($P < 0.05$, Figure 2E), with efficacy comparable to 5-ASA ($P > 0.05$). Furthermore, $GSNS_M$ and $GSNS_H$ treatments significantly reversed colon shortening ($P < 0.001$, Figure 2C), demonstrating a dose-dependent protective effect on colonic structure.

Modulation of inflammatory and oxidative stress biomarkers by GSNS in Serum and Colon

We confirmed the successful induction of the UC model based on a significant rise in pivotal pro-inflammatory cytokines [31]. As illustrated in Figures 3A - D, DSS induction resulted in a substantial increase ($p < 0.001$) in TNF-α, IL-6, and IL-1β levels in both serum and colon tissue. It also altered IL-10 expression, an anti-inflammatory cytokine. Administration of GSNS and 5-ASA significantly reversed these aberrant cytokine profiles ($p < 0.05$, $p < 0.01$, or $p < 0.001$). The suppressive effect of GSNS on pro-inflammatory cytokines was dose-dependent, with the high-dose group exhibiting efficacy comparable to the 5-ASA group. Furthermore, data on colonic oxidative stress markers (Figures 3E - H) showed that GSNS reduced MPO activity and MDA content in a dose-dependent manner, while enhancing SOD activity and GSH levels. This antioxidant effect was most pronounced at the $GSNS_H$, equivalent to that achieved with 5-ASA treatment.

Histopathology of colon tissue and immunohistochemical analysis of Nrf2 Protein *Expression*

Colon tissue H&E staining results and pathological scores are shown in Figure 4A and C. The control group displayed preserved colonic architecture, characterized by an intact mucosal layer and regularly arranged glands. Inflammatory cells were only sporadically present in the lamina propria. In contrast, the model group displayed typical pathological features of severe UC: extensive mucosal epithelial defects, substantial depletion of goblet cells, destruction and loss of crypt architecture, severe submucosal oedema, and transmural infiltration by a large number of inflammatory cells ($P < 0.001$ vs. control group) [32]. GSNS treatment improved these pathological injuries in a dose-dependent manner. Compared with the model group, the $GSNS_M$ and $GSNS_H$ groups showed significantly reduced inflammatory infiltration and improved mucosal architecture ($p < 0.001$). Notably, the overall histopathological score in the $GSNS_H$ group was not significantly different from that in the 5-ASA group ($p > 0.05$), indicating a similar degree of improvement.

The IHC results presented in Figure 4B and D - F demonstrate that, compared with the control group, the DSS model group showed significantly reduced positive area ratio, areal density, and nuclear positive expression intensity (H-Score) of the Nrf2 protein in colon tissue ($p < 0.001$ for each). The decrease in the nuclear H-Score, in particular, indicated impaired nuclear translocation of Nrf2. Following GSNS intervention, the positive area ratio, areal density, and nuclear H-Score of Nrf2 increased in a dose-dependent manner in the $GSNS_M$ and $GSNS_H$ groups. The extent of recovery in the $GSNS_H$ group was equivalent to that in the 5-ASA group, with no statistically significant difference [33-35]. These results confirm, at the tissue level, that GSNS can effectively promote the expression and nuclear translocation of Nrf2 in colon tissue, thereby activating the Nrf2 signalling pathway.

Immunofluorescence analysis of desmoglein in the colon

Figure 5A presents representative immunofluorescence images depicting the localization of ZO-1 and Occludin [36]. In the control group, both proteins exhibited continuous, distinct, linear distribution along the colonic epithelial cell membrane.

Citation: Lyu X, Zhang L, Si J, Dai S, Su H, Lyu S, et al. Activation of the Nrf2 Signaling Pathway by a Ginseng-Salvia-Notoginseng Composite Alleviates Ulcerative Colitis via Restoring Gut Microbiota and Intestinal Barrier. Adv Appl of Bioengine. 2026; 2(1): 004-017. Available from: https://dx.doi.org/10.17352/aabe.000003

Table 2: Chemical compositions of GSNS

NO	Name	Formula	Mass(Da)	Measured m/z	Error (ppm)	Rt (min)	Score	Polarity Mode
1	20(S)-Ginsenoside Ck	$C_{36}H_{62}O_8$	644.42394	645.43122	2.5	73.558	80.1	Positive
2	Apigenin-7-O-β-D-glucoside	$C_{21}H_{20}O_{10}$	432.10527	433.11255	0.8	38.479	85.2	Positive
3	Cimifugin	$C_{15}H_{10}O_4$	306.11	307.11728	0.65	58.765	83.4	Positive
4	Cryptotanshinone	$C_{16}H_{18}O_6$	296.14109	297.14837	1.1	34.799	90.7	Positive
5	Ginsenoside Rk1	$C_{19}H_{20}O_3$	766.48583	767.49311	0.52	70.74	88.8	Positive
6	Pseudoginsenoside F11	$C_{42}H_{70}O_{12}$	800.49144	801.49872	1.17	71.467	81.2	Positive
7	Tanshinone IIA	$C_{42}H_{72}O_{14}$	294.12515	295.13243	0.96	58.234	90.9	Positive
8	20(R)-Ginsenoside Rg2	$C_{42}H_{72}O_{13}$	784.49824	785.50552	1.2	61.71	84	Negative
9	20(R)-Notoginsenoside R2	$C_{41}H_{70}O_{13}$	770.48215	771.48943	0.65	60.069	81.1	Negative
10	Chikusetsu saponin IVa	$C_{42}H_{66}O_{14}$	1588.89248	1589.89976	1	72.926	87.4	Negative
11	Cynaroside	$C_{21}H_{20}O_{11}$	448.09996	449.10724	1.3	39.605	80.6	Negative
12	Ginsenoside F1	$C_{36}H_{62}O_9$	684.44514	685.45242	2.9	65.117	85.1	Negative
13	Ginsenoside F2	$C_{42}H_{72}O_{13}$	830.50392	831.5112	2.8	75.861	87	Negative
14	Ginsenoside Rb1	$C_{54}H_{92}O_{23}$	2217.20669	2218.21397	1.1	68.951	80.6	Negative
15	Ginsenoside Rb2	$C_{53}H_{90}O_{22}$	2157.18472	2158.192	2.5	69.6	80	Negative
16	Ginsenoside Rc	$C_{53}H_{90}O_{22}$	1124.59903	1125.60631	2.4	71.066	81.9	Negative
17	Ginsenoside Rd	$C_{48}H_{82}O_{18}$	1893.10098	1894.10826	1.6	73.504	82.4	Negative
18	Ginsenoside Re	$C_{48}H_{82}O_{18}$	992.5561	993.56339	1.4	50.336	89.2	Negative
19	Ginsenoside Rf	$C_{42}H_{72}O_{14}$	800.49283	801.50011	0.78	59.247	83.2	Negative
20	Ginsenoside Rg1	$C_{42}H_{72}O_{14}$	846.49891	847.50619	1.5	63.744	81.3	Negative
21	Ginsenoside Rg2	$C_{42}H_{72}O_{13}$	830.50435	831.51163	1.56	57.455	80.9	Negative
22	Ginsenoside Rg3	$C_{42}H_{72}O_{13}$	784.4987	785.50598	1.78	75.298	86.7	Negative
23	Ginsenoside Ro	$C_{48}H_{76}O_{19}$	1912.99893	1914.00621	1.02	69.874	80.4	Negative
24	Notoginsenoside Fe	$C_{47}H_{80}O_{17}$	962.54677	963.55405	2.52	78.006	81	Negative
25	Notoginsenoside R1	$C_{47}H_{80}O_{18}$	1865.07046	1866.07774	1.6	49.023	80.6	Negative

In the DSS model group, this linear fluorescence signal was significantly attenuated and interrupted, indicating severe disruption of tight junction structures. GSNS treatment restored the continuous membrane localization of ZO-1 and Occludin in a dose-dependent manner, with gradual improvement in fluorescence signal intensity and continuity. In the $GSNS_H$ group, the distribution patterns of both proteins recovered to a state similar to that of the 5-ASA group, visually confirming GSNS's effective repair of the intestinal physical barrier.

Transmission electron microscopy analysis of the ultrastructure of the colon epithelium

Representative transmission electron micrographs of colonic tissue are shown in Figure 5B. Examination by TEM revealed that control intestinal epithelial cells were characterized by dense, orderly microvilli, intact tight and gap junctions, and normal organelle structure. The DSS model group demonstrated severe ultrastructural damage: sparse or shed microvilli, widened intercellular spaces, blurred or absent tight junctions, and swollen, vacuolated mitochondria [37]. Following GSNS treatment, epithelial ultrastructure exhibited dose-dependent repair. In the $GSNS_H$ group, intestinal epithelial microvillus density, cell junction integrity, and organelle status all approached normal levels, comparable to the 5-ASA group.

GSNS enhances antioxidant and barrier functions at the genetic and protein levels

Western blot analysis results for protein expression are presented in Figure 6A, and corroborate the corresponding gene-level changes. A marked reduction was observed in the expression of Occludin, Nrf2, and its downstream effector HO-1 in the model group [38]. Following GSNS treatment, the protein expression levels of all three targets were significantly increased. Furthermore, the band intensity analysis histograms in Figure 6B - D revealed significant differences between the DSS model group and both the control group and the $GSNS_H$ group ($p < 0.001$). The RT-qPCR results shown in Figure 6E - H indicated that DSS-induced colitis significantly upregulated Keap1 mRNA and miR-146a-5p expression in colon tissue ($p < 0.001$), while suppressing the expression of the antioxidant gene GCLC and the transcription factor SXRN1. GSNS intervention reversed these abnormal expressions in a dose-

Citation: Lyu X, Zhang L, Si J, Dai S, Su H, Lyu S, et al. Activation of the Nrf2 Signaling Pathway by a Ginseng-Salvia-Notoginseng Composite Alleviates Ulcerative Colitis via Restoring Gut Microbiota and Intestinal Barrier. Adv Appl of Bioengine. 2026; 2(1): 004-017. Available from: https://dx.doi.org/10.17352/aabe.000003

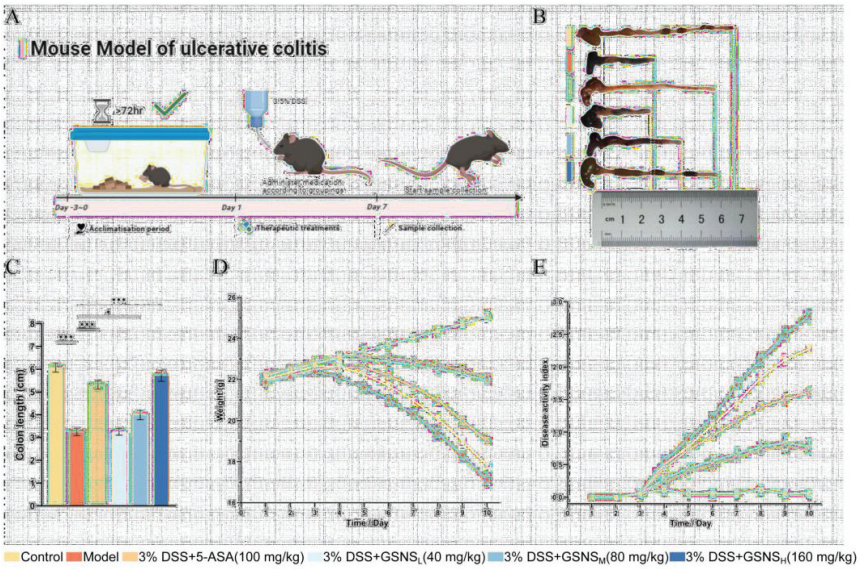

Figure 2: Therapeutic effects of GSNS on DSS-induced UC in mice. (A) Schematic diagram of the experimental design and treatment timeline. (B) Representative macroscopic photographs of colon tissues from each group. (C) Measurement results of colon length. (D) Body weight change curves during the treatment period. (E) DAI scores. Data are expressed as the mean ± SEM (n = 6). Statistical significance: *p < 0.05, ***p < 0.001 compared with the Model group.

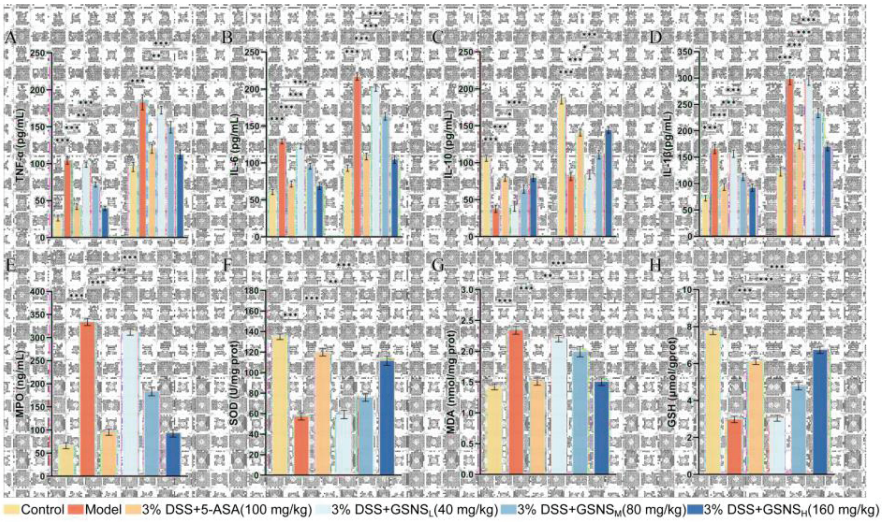

Figure 3: Modulation of Inflammatory and Oxidative Stress Profiles by GSNS in Mice with UC.(A - D) Panels show GSNS effects on TNF-α, IL-6, IL-10, and IL-1β levels in both colon tissue and serum (n = 6). (E - H) Panels show GSNS effects on serum markers of oxidative stress: MPO, SOD, MDA, and GSH (n = 6). Statistical significance relative to the Model group is indicated: *p < 0.05, **p < 0.01, ***p < 0.001.

dependent manner. In summary, this study demonstrates, at both transcriptional and translational levels, that GSNS alleviates colitis by inhibiting Keap1, promoting Nrf2 nuclear translocation, and subsequently upregulating downstream antioxidant protein HO-1 and barrier protein Occludin.

Furthermore, its regulation of relevant miRNAs, such as miR-146a-5p, highlights its multi-level, synergistic mechanism of action.

Analysis of gut microbiota changes following GSNS Treatment

The effect of GSNS on the gut microbiota in DSS-colitis mice was examined by 16S rRNA gene sequencing of cecal contents; a Venn diagram was generated to visualize OTU overlap, showing common and group-specific microbial features. The Venn diagram analysis revealed the compositional characteristics of OTU distribution across groups (Figure 7A). The proportions of unique OTUs in the control, model, and GSNS$_H$ groups were 20.3%, 11.8%, and 7.19%, respectively, indicating that each group harbored a certain proportion of unique microbial taxa. Intergroup comparisons revealed the lowest OTU overlap between the control and model groups (2.61%), indicating that DSS modelling significantly altered the fundamental composition of the gut microbiota. The GSNS$_H$ group showed 7.84% OTU overlap with the control group and 10.5% with the model group, suggesting that the microbiota structure after GSNS intervention retained features

Citation: Lyu X, Zhang L, Si J, Dai S, Su H, Lyu S, et al. Activation of the Nrf2 Signaling Pathway by a Ginseng-Salvia-Notoginseng Composite Alleviates Ulcerative Colitis via Restoring Gut Microbiota and Intestinal Barrier. Adv Appl of Bioengine. 2026; 2(1): 004-017. Available from: https://dx.doi.org/10.17352/aabe.000003

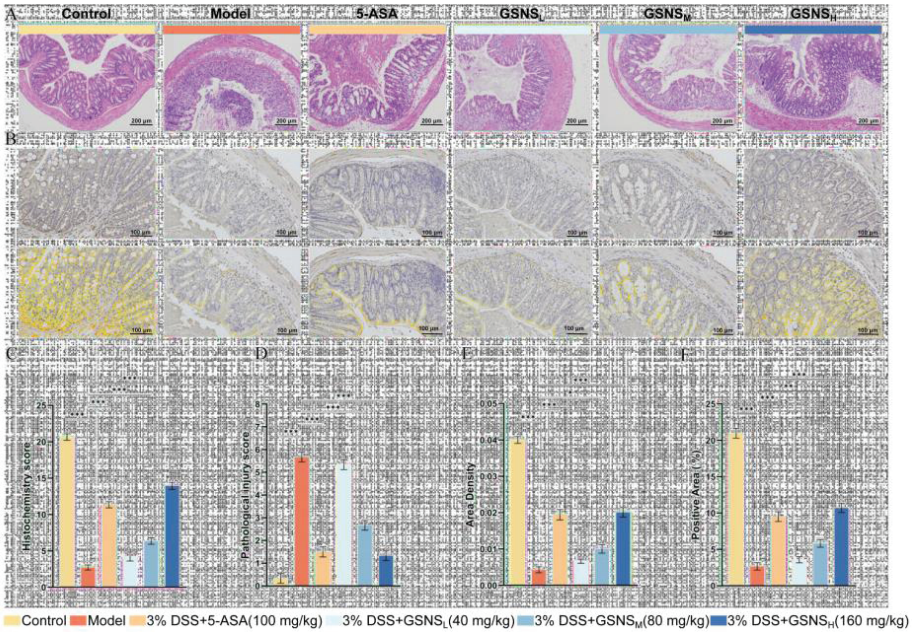

Figure 4: Histopathological evaluation and Nrf2 expression in colonic tissues of DSS-induced colitis mice treated with GSNS. (A) Representative H&E-stained sections of colon tissues (scale bar, 200 μm). (B) Representative immunohistochemical staining images showing Nrf2 expression in colon tissues (scale bar, 100 μm). (C) Histopathological injury scores. (D) Immunohistochemical scores for Nrf2 expression. (E) Quantitative analysis of the Nrf2-positive area ratio. (F) Quantitative analysis of the Nrf2-positive area density. *p < 0.05, **p < 0.01, ***p < 0.001 compared with the model group. The results are expressed as mean ± SEM.

characteristic of both normal and diseased states. Furthermore, the OTUs shared among the three groups accounted for the highest proportion (39.9%), indicating a core microbiota that remains relatively stable under experimental conditions. These findings demonstrate that DSS intervention significantly alters microbial composition, while GSNS treatment partially restores structural features resembling those of normal microbiota. Assessment of microbial community structure differences between groups via beta diversity analysis revealed significant segregation in Bray-Curtis and Jaccard distance principal coordinate analysis (Figure 7B - C) [39,40]. Samples from the GSNS intervention group exhibited distribution patterns closer to the normal control group. Further assessment of intra-group microbial diversity was performed via alpha diversity analysis using multiple indices (Chao1, Shannon, Simpson, richness, and Pielou's evenness; Figure 7D - H). The results consistently showed that DSS modeling significantly reduced both microbial richness and evenness in the gut. In contrast, GSNS treatment restored these diversity metrics in a dose-dependent manner, with the most pronounced recovery observed in the GSNS$_H$ group. At the phylum level, DSS induction led to a decreased relative abundance of Firmicutes and an increase in Bacteroidetes, a trend that was reversed upon GSNS treatment. This community structure analysis across phylum, family, and genus levels is presented in bar charts (Figure 7I - K), where each bar represents one sample, colors denote different taxa, and the vertical axis shows relative abundance.

LEfSe was employed to identify species with significant intergroup differences (LDA score > 3.5) [41], with the results visualized in Figure 7L, M. Across the four groups at the phylum and genus levels, a total of 30 discriminant taxonomic groups were identified: 18 in the control group, 7 in the model group, and 5 in the GSNS$_H$ group. Key taxonomic units with significantly different abundances in the control group gut microbiota included: Muribaculaceae, Oscillospirales, Oscillospiraceae, Ruminococcaceae, Ruminococcus, Oscillibacter, Muribaculum, Colidextribacter, the [*Eubacterium*] coprostanoligenes group (at both family and genus levels), and the genus *Roseburia*. Key taxonomic units significantly enriched in the gut microbiota of the model group included: the phylum Proteobacteria, Gammaproteobacteria, Bacteroidaceae, *Bacteroides*, Enterobacterales, Enterobacteriaceae, and *Escherichia-Shigella*. Key taxonomic units significantly enriched in the GSNS$_H$ group gut microbiota were: Prevotellaceae, Prevotellaceae_UCG-001, and Alphaproteobacteria. The enrichment of these groups may reflect the specific regulatory effects of GSNS intervention on microbial community structure and is associated with improvements in intestinal function.

Furthermore, Spearman correlation network analysis revealed alterations in microbial interactions. Results showed that in the model group, gut microbiota exhibited a disordered interaction pattern centered on inflammation-associated groups such as Proteobacteria. Following GSNS intervention, microbial network structure underwent significant remodeling: not only was positive synergy enhanced among beneficial groups like *Lactobacillus* and *Dubosella*, but their associations with opportunistic pathogens such as Enterobacteriaceae were also weakened. Concurrently, the interaction patterns of groups labeled "positively correlated" in Figure 7 - N, such as the phylum Cyanobacteria, became more stable. This further enhanced overall network complexity and structural stability. These findings indicate that GSNS not only restores gut microbiota balance at the diversity and community structure levels but also enhances ecological network stability by

Citation: Lyu X, Zhang L, Si J, Dai S, Su H, Lyu S, et al. Activation of the Nrf2 Signaling Pathway by a Ginseng-Salvia-Notoginseng Composite Alleviates Ulcerative Colitis via Restoring Gut Microbiota and Intestinal Barrier. Adv Appl of Bioengine. 2026; 2(1): 004-017. Available from: https://dx.doi.org/10.17352/aabe.000003

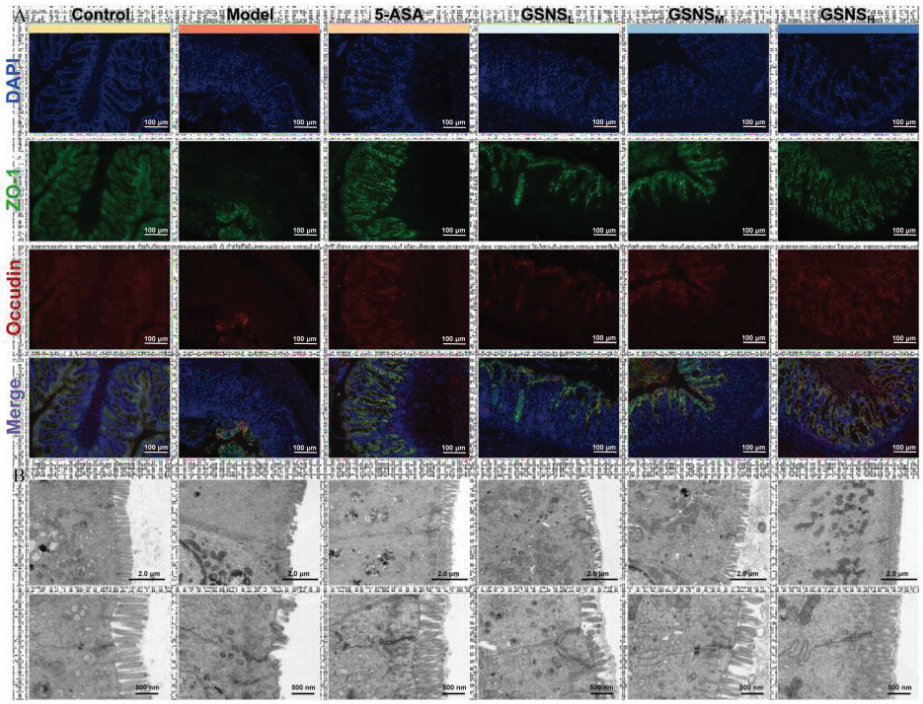

Figure 5: Effects of GSNS on colonic epithelial barrier integrity. (A) Localization of the tight junction proteins ZO-1 (green) and Occludin (red) in colon tissues across the six experimental groups is shown in representative immunofluorescence images. Nuclei are counterstained with DAPI (blue). (B) Representative TEM images depicting the ultrastructure of colonic epithelial tight junctions.

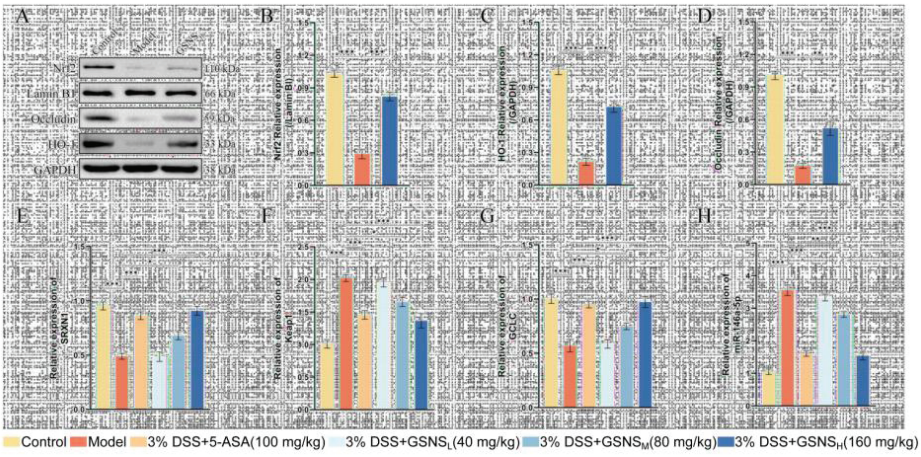

Figure 6: GSNS alleviated colitis and modulated the expression of associated proteins and genes in DSS-induced UC mice. (A) Representative protein bands of nuclear Nrf2, HO-1, and Occludin (n = 3). (B - D) Histograms depicting the band intensity analysis of nuclear Nrf2, HO-1, and Occludin. (E - G) Expression levels of mRNA genes SRXN1, Keap1, and GCLC in each group. (H) Expression level of the miRNA gene miR-146a-5p in each group. *p < 0.05, **p < 0.01, *** p < 0.001 versus the Model group. Significant differences (p < 0.001) were observed in the GSNSH treatment group compared to the Model group. Data are expressed as mean ± SEM (n = 3).

reconfiguring beneficial microbial collaborations. This systemic approach supports the improvement of the pathological state of colitis.

Discussion

A DSS-induced mouse model of UC was employed to evaluate the therapeutic potential and mechanistic basis of the GSNS. Integrated pharmacodynamic, molecular, and microbiome analyses demonstrate that GSNS significantly alleviates disease severity. Its beneficial actions appear to be mediated through a multi-targeted mechanism involving suppression of systemic and local inflammation, activation of the Nrf2/HO-1 pathway to mitigate oxidative stress, enhancement of intestinal barrier integrity, and restoration of gut microbiota homeostasis. These findings collectively support that GSNS exerts its protective effect via a coordinated modulation of the inflammation, oxidative stress, barrier, and microbiota axis.

In terms of anti-inflammatory and antioxidant effects, the pharmacodynamic findings of this study corroborate the mechanisms of action reported in the literature for the active

Citation: Lyu X, Zhang L, Si J, Dai S, Su H, Lyu S, et al. Activation of the Nrf2 Signaling Pathway by a Ginseng-Salvia-Notoginseng Composite Alleviates Ulcerative Colitis via Restoring Gut Microbiota and Intestinal Barrier. Adv Appl of Bioengine. 2026; 2(1): 004-017. Available from: https://dx.doi.org/10.17352/aabe.000003

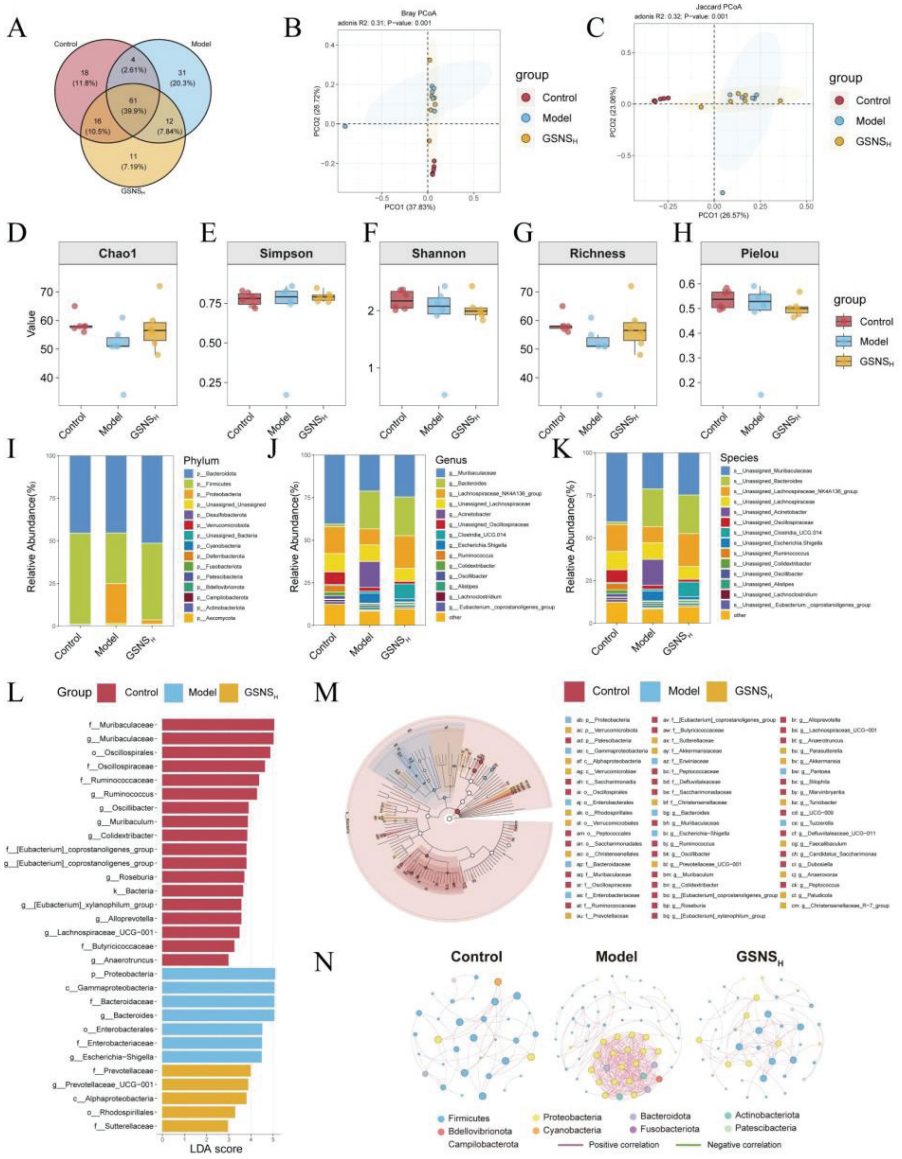

Figure 7: Analysis of intestinal contents via 16S rRNA gene sequencing reveals the modulatory effect of GSNS on DSS-induced microbiota dysbiosis. (A) Venn diagram of group-specific and shared ASVs; (B, C) PCoA based on Bray-Curtis and Jaccard distances. Alpha diversity indices: (D) Chao1, (E) Simpson, (F) Shannon, (G) Richness, and (H) Pielou's evenness. Microbial community composition at the (I) phylum, (J) family, and (K) genus levels. (L) Histogram of LDA scores representing significantly discriminant taxa across groups. (M) Cladogram generated by LEfSe analysis illustrating the phylogenetic distribution of discriminant taxa. (N) Spearman correlation-based network analysis of microbial interactions. The results are expressed as mean ± SEM (n = 6).

components of individual herbs [16-18]. As shown in Figures 2 - 4, GSNS intervention dose dependently improved DSS-induced weight loss, colon length, and alleviated histopathological damage, while significantly reducing levels of pro-inflammatory factors (TNF-α, IL-6, and IL-1β). These effects align with established reports that ginsenosides, danenol, and notoginsenosides suppress inflammation by modulating the NF-κB pathway [42-44]. Crucially, immunohistochemical and molecular biological analyses further revealed GSNS's direct antioxidant mechanism: it significantly promoted Nrf2 protein expression and nuclear translocation in colonic tissue (Figure 4) while upregulating the downstream antioxidant protein HO-1. This in situ evidence confirms that GSNS effectively retains and integrates the core activity of its constituent herbs, bolstering cellular antioxidant defenses via activation of the Nrf2/HO-1 signaling axis [45,46].

This research demonstrates that GSNS, particularly at a $GSNS_H$, achieved comparable improvement levels to the 5-ASA group in key parameters, including DAI, colon length restoration, and histopathological score. The comprehensive restorative effect observed in the whole animal model suggests potential synergistic interactions among the multiple components within this compound formulation [47-49]. The enhanced overall efficacy is likely due to the distinct active constituents of ginseng, salvia, and notoginseng acting on interrelated pathological pathways, such as inflammation, oxidative stress, and barrier repair, which ultimately converge to form a more robust, multi-target therapeutic network [50-52]. This amplifies the contributions of individual herbs and exemplifies the holistic regulatory characteristics of traditional Chinese medicine formulas.

Citation: Lyu X, Zhang L, Si J, Dai S, Su H, Lyu S, et al. Activation of the Nrf2 Signaling Pathway by a Ginseng-Salvia-Notoginseng Composite Alleviates Ulcerative Colitis via Restoring Gut Microbiota and Intestinal Barrier. Adv Appl of Bioengine. 2026; 2(1): 004-017. Available from: https://dx.doi.org/10.17352/aabe.000003

At the molecular level, this study further revealed the regulatory effect of GSNS on the Nrf2 signaling pathway. Enhanced nuclear translocation of Nrf2 was observed following GSNS treatment, along with upregulated expression of its downstream effector HO-1 and the tight junction protein Occludin in colon tissues, as determined by Western blot. These changes were consistent with transcriptional alterations: RT-qPCR results confirmed that GSNS downregulated Keap1 mRNA expression while upregulating antioxidant genes GCLC and Srxn1 [53-55]. Furthermore, GSNS restored the abnormally elevated level of miR-146a-5p, a miRNA involved in inflammatory feedback regulation, in DSS-induced mice to near-normal levels [56]. These data suggest that GSNS sustains activation of the Nrf2/HO-1 antioxidant axis by inhibiting Keap1 and may further facilitate inflammation resolution by regulating miR-146a-5p. Notably, the activation of antioxidant signaling and the enhancement of epithelial barrier function exhibited synchronous and dose-dependent responses, indicating that GSNS coordinates key pathways such as Nrf2 to synergistically restore intracellular redox balance and physical barrier integrity.

To elucidate the regulatory effects of GSNS on gut microbiota, 16S rRNA gene sequencing was performed in DSS-induced UC mice [57,58]. Venn analysis indicated a marked alteration in microbial composition following DSS induction, with only 2.61% of OTUs shared between the control and model groups. After GSNS intervention, the overlap with the control group increased to 7.84%, suggesting a partial restoration of microbial structure. Alpha diversity indices, including Chao1 and Shannon, demonstrated that GSNS dose-dependently recovered the DSS-induced reduction in microbial richness and evenness. Beta diversity analysis further supported that GSNS treatment shifted the microbial community closer to that of the control group, as measured by Bray-Curtis and Jaccard distances. At the phylum level, GSNS significantly mitigated the DSS-induced dysbiosis, particularly by restoring the Firmicutes/Bacteroidetes ratio. LEfSe analysis revealed that GSNS downregulated pro-inflammatory taxa enriched in the model group, such as Proteobacteria, Enterobacteriaceae, and *Escherichia-Shigella*, while promoting beneficial genera including Prevotellaceae. Importantly, Spearman correlation network analysis showed that GSNS remodeled microbial interactions: the Proteobacteria-centered network observed in the model group was replaced, positive correlations among beneficial bacteria, such as *Lactobacillus*, were strengthened, and overall network complexity and stability were enhanced. In summary, GSNS not only rectifies compositional imbalances in the gut microbiota but also fosters a healthier ecological network, highlighting its role in restoring intestinal microenvironment homeostasis and showing its therapeutic potential in UC.

The findings of this study demonstrate that GSNS alleviates colitis by synergistically activating the Nrf2/HO-1 antioxidant pathway, repairing epithelial tight junctions, and reshaping the gut microbiota. This provides an integrated therapeutic model with a clear multi-target mechanism for complex diseases such as UC, which are characterized by a vicious cycle of oxidative stress, barrier disruption, and dysbiosis. [59-61]. The mode of action of GSNS suggests that its components may act synergistically or through additive effects at the host-microbiota interface to restore intestinal homeostasis more effectively.

However, as a preclinical study, translation to human applications requires further validation [62]. The optimal dosage, long-term safety, and pharmacokinetic profile of GSNS in humans remain to be determined. Moreover, while synchronous improvements across pathways were observed, their temporal and causal relationships are not fully resolved. Future studies are needed to distinguish whether microbiota alterations are primary or secondary to the therapeutic effects of GSNS. Approaches such as using germ-free animals, performing fecal transplants, or isolating specific constituents could help clarify these mechanistic nuances. In addition, the specific chemical constituents responsible for the antioxidant, anti-inflammatory, and microbiota-modulating effects of GSNS need to be identified through compound isolation and reconstitution experiments [63]. Current analyses based on 16S rRNA sequencing primarily provide information on microbial community structure. A multi-omics approach encompassing metagenomics, metabolomics, and transcriptomics is warranted to delineate the specific interactions among microbial genes, metabolites, and host pathways, and to fully decipher the comprehensive regulatory network orchestrated by GSNS [64].

In summary, this work systematically delineates the multi-target, multi-dimensional action framework of GSNS in UC, offering empirical support for the "multi-component-multi-target-multi-pathway" paradigm of herbal formulations in treating complex diseases. It lays a foundation for developing innovative strategies aimed at holistically restoring intestinal homeostasis. Future efforts should focus on identifying active components, elucidating mechanistic causality, and advancing clinical translation to provide UC patients with a potential therapy possessing systemic regulatory benefits.

Conclusions

In conclusion, this study demonstrates that the GSNS alleviates UC through a multi-target mechanism. GSNS exerts its effects by activating the Nrf2 signaling pathway to combat oxidative stress and inflammation, restoring intestinal barrier integrity via Occludin upregulation and preservation of tight junction ultrastructure (as confirmed by TEM), and modulating gut microbiota homeostasis. Collectively, the therapeutic outcome arises from the synergistic regulation of interconnected antioxidant, anti-inflammatory, barrier-repair, and microbial-modulating pathways. These findings provide modern pharmacological validation for the application of this traditional Chinese medicine formulation in UC management, highlighting activation of the Nrf2 signaling pathway as a central mechanism underlying its multi-target efficacy.

Citation: Lyu X, Zhang L, Si J, Dai S, Su H, Lyu S, et al. Activation of the Nrf2 Signaling Pathway by a Ginseng-Salvia-Notoginseng Composite Alleviates Ulcerative Colitis via Restoring Gut Microbiota and Intestinal Barrier. Adv Appl of Bioengine. 2026; 2(1): 004-017. Available from: https://dx.doi.org/10.17352/aabe.000003

Author contributions

Software, X.L. (Xinao Lyu), L.Z., S.D., and S.L.; Formal analysis, X.L. (Xinao Lyu), H.S., and L.C.; Investigation, X.L. (Xinao Lyu), S.D., and J.S.; Data curation, X.L. (Xinao Lyu) and L.Z. (Liurong Zhang); Writing—original draft, X.L. (Xinao Lyu) and L.Z.; Writing—review & editing, H.L.; Funding acquisition, X.J. All authors have read and agreed to the published version of the manuscript.

Funding

This research was supported by grants from the Jilin Provincial Department of Education Scientific Research Project. Development Plan Project: JJKH20250214CY.

Institutional review board statement

This study was approved by the Institutional Animal Care and Use Committee of Jilin University School of Pharmaceutical Science (No. 20250121 and Approval Date: 22 August 2025).

Data availability statement

The original contributions presented in this study are included in the article/Supplementary Material. Further inquiries can be directed to the corresponding authors.

Disclaimer/Publisher's Note

The statements, opinions, and data contained in all publications are solely those of the individual author(s) and contributor(s) and not of MDPI and/or the editor(s). MDPI and/or the editor(s) disclaim responsibility for any injury to people or property resulting from any ideas, methods, instructions, or products referred to in the content.

References

1. Damianos JA, Osikoya O, Brennan G. Upadacitinib for acute severe ulcerative colitis: a systematic review. Inflamm Bowel Dis. 2025;31:1145–1149. doi:10.1093/ibd/izae191. Available from: https://doi.org/10.1093/ibd/izae191

2. Yuan S, Cai L, Su M. Natural antioxidant substances improve oxidative stress and alleviate ulcerative colitis: a meta-analysis of randomized controlled trials. Sci Rep. 2025;15:45636. Available from: https://www.nature.com/articles/s41598-025-30617-x

3. Gaidos JKJ, Hashash JG. Monitoring inflammatory bowel disease activity: when, how, and why. Am J Gastroenterol. 2025;120:1732–1741. Available from: https://doi.org/10.14309/ajg.0000000000003582

4. Bu F, Chen K, Chen S, Jiang Y. Gut microbiota and intestinal immunity interaction in ulcerative colitis and its application in treatment. Front Cell Infect Microbiol. 2025;15:1565082. Available from: https://doi.org/10.3389/fcimb.2025.1565082

5. Bamias G, Menghini P, Pizarro TT, Cominelli F. Targeting TL1A and DR3: the new frontier of anti-cytokine therapy in IBD. Gut. 2025;74:652–668. Available from: https://doi.org/10.1136/gutjnl-2024-332504

6. Sandle GI, Rajendran VM. Ion transport and epithelial barrier dysfunction in experimental models of ulcerative colitis. Am J Physiol Gastrointest Liver Physiol. 2025;328:G811–G830. Available from: https://doi.org/10.1152/ajpgi.00204.2024

7. Wu H, Li YL, Wang Y, Wang YG, Hong JH, Pang MM, Liu PM, Yang JJ, et al. Anemoside B4 alleviates ulcerative colitis by attenuating intestinal oxidative stress and NLRP3 inflammasome via activating aryl hydrocarbon receptor through remodeling the gut microbiome and metabolites. Redox Biol. 2025;85:103746. Available from: https://doi.org/10.1016/j.redox.2025.103746

8. Lu X, Sun Y, Zhang Z, Sun Z, Wang S, Xu E. Regulation of pyroptosis by natural products in ulcerative colitis: mechanisms and therapeutic potential. Front Pharmacol. 2025;16:1573684. Available from: https://doi.org/10.3389/fphar.2025.1573684

9. Wan L, Qian C, Yang C, Peng S, Dong G, Cheng P, et al. Ginseng polysaccharides ameliorate ulcerative colitis via regulating gut microbiota and tryptophan metabolism. Int J Biol Macromol. 2024;265:130822. Available from: https://doi.org/10.1016/j.ijbiomac.2024.130822

10. Zeng L, Li X, Bai G, Liu Y, Lu Q. Rectal administration of Panax notoginseng and Colla Corii Asini suppositories in ulcerative colitis: clinical effect and influence on immune function. Am J Transl Res. 2022;14:603–611. Available from: https://pubmed.ncbi.nlm.nih.gov/35173878/

11. Peng KY, Gu JF, Su SL, Zhu Y, Guo JM, Qian D, et al. Salvia miltiorrhiza stems and leaves total phenolic acids combination with tanshinone protect against DSS-induced ulcerative colitis through inhibiting TLR4/PI3K/AKT/mTOR signaling pathway in mice. J Ethnopharmacol. 2021;264:113052. Available from: https://doi.org/10.1016/j.jep.2020.113052

12. Li W, Wang Y, Zhang Y, Fan Y, Liu J, Zhu K, et al. Lizhong decoction ameliorates ulcerative colitis by inhibiting ferroptosis of enterocytes via the Nrf2/SLC7A11/GPX4 pathway. J Ethnopharmacol. 2024;326:117966. Available from: https://doi.org/10.1016/j.jep.2024.117966

13. Song Y, Lin R, Fu Y, Wang A, Yang H, Liu W. Ameliorative effects and mechanism of Panax notoginseng extract on ulcerative colitis mice based on a multi-omics strategy. Front Immunol. 2025;16:1727993. Available from: https://doi.org/10.3389/fimmu.2025.1727993

14. Yu J, Mei W, Zhu J, Wang Z, Liu X, Zhou R, et al. Aurantii Fructus extract alleviates DSS-induced colitis in mice via regulating NF-κB and Nrf2/HO-1 signaling pathways and modulating intestinal microbiota. Front Nutr. 2025;12:1661040. Available from: https://doi.org/10.3389/fnut.2025.1661040

15. Stojanovic B, Milivojcevic Bevc I, Dimitrijevic Stojanovic M, Stojanovic BS, Jovanovic M, Lazarevic S, et al. Nrf2 as a molecular guardian of redox balance and barrier integrity in IBD. Antioxidants (Basel). 2025;14. Available from: https://doi.org/10.3390/antiox14121407

16. Tan L, Li Z, Wu J, Liu H, Yang T, Wang J, et al. Ginsenoside Rk2 provides multidimensional relief for ulcerative colitis by improving intestinal barrier function, reshaping gut microbiota, and regulating Th17/Treg balance. J Agric Food Chem. 2025;73:25340–25357. Available from: https://doi.org/10.1021/acs.jafc.5c04210

17. Wang C, Liu H, Li Z, Yang Q, Wang Q, Yang T, et al. Oleanolic acid 28-O-β-D-glucopyranoside: a novel therapeutic agent against ulcerative colitis via anti-inflammatory, barrier-preservation, and gut microbiota-modulation. Biomed Pharmacother. 2024;180:117534. Available from: https://doi.org/10.1016/j.biopha.2024.117534

18. Zhang J, Xie J, Niu Z, You L, Liu Y, Guo R, et al. Ginsenoside Rg2, a principal effective ingredient of Panax ginseng, attenuates DSS-induced ulcerative colitis through the NF-κB/NLRP3 pathway. J Ginseng Res. 2025;49:282–293. Available from: https://doi.org/10.1016/j.jgr.2025.02.001

19. Ahmadi A, Shokoohizadeh L, Sheikhesmaili F, Mirzaei MK, Mohammadi A, Nikkhoo B, et al. Gut microbiomes and treatment-resistant ulcerative colitis: a case-control study using qPCR. BMC Microbiol. 2025;25:254. Available from: https://doi.org/10.1186/s12866-025-03963-z

Citation: Lyu X, Zhang L, Si J, Dai S, Su H, Lyu S, et al. Activation of the Nrf2 Signaling Pathway by a Ginseng-Salvia-Notoginseng Composite Alleviates Ulcerative Colitis via Restoring Gut Microbiota and Intestinal Barrier. Adv Appl of Bioengine. 2026; 2(1): 004-017. Available from: https://dx.doi.org/10.17352/aabe.000003

20. Zhang M, Liu R, Zhou T, Guo Y, Li H, Wu W. Exploring the anti-fatigue properties of ginseng stem and leaf saponins: using UHPLC-MS metabolomics and neurotransmitter analysis. Phytomedicine. 2025;139:156459. Available from: https://doi.org/10.1016/j.phymed.2025.156459

21. Hubrecht RC, Carter E. The 3Rs and humane experimental technique: implementing change. Animals (Basel). 2019;9. Available from: https://doi.org/10.3390/ani9100754

22. Cooper HS, Murthy SN, Shah RS, Sedergran DJ. Clinicopathologic study of dextran sulfate sodium experimental murine colitis. Lab Invest. 1993;69:238–249. Available from: https://pubmed.ncbi.nlm.nih.gov/8350599/

23. Liu Y, Huang J, Yu J, Fu L, Huang R, Liu J, et al. Curcumin modulates TIGIT/Neuropilin-1 to regulate T-cell immune homeostasis in ulcerative colitis. Foods. 2025;14. Available from: https://doi.org/10.3390/foods14244323

24. Zhang L, Wang Z, Li S, Liu X, Xu C, Li L. The potential roles of CHI3L1 in failed autologous arteriovenous fistula in end-stage renal disease. Tohoku J Exp Med. 2023;259:253–261. Available from: https://doi.org/10.1620/tjem.2022.j120

25. Hong CE, Lyu SY. Immunomodulatory activities of emerging rare ginsenosides F1, Rg5, Rk1, Rh1, and Rg2: from molecular mechanisms to therapeutic applications. Pharmaceuticals (Basel). 2025;18. Available from: https://doi.org/10.3390/ph18101529

26. Song Y, Zhang X, Han X, Wang G, Wang M, Wu H, et al. Ginsenoside Rb1 alleviates blood-brain barrier damage and demyelination in experimental autoimmune encephalomyelitis mice by regulating JNK/ERK/NF-κB signaling pathway. J Ethnopharmacol. 2025;343:119448. Available from: https://doi.org/10.1016/j.jep.2025.119448

27. Lu K, Xia Y, Cheng P, Li Y, He L, Tao L, et al. Synergistic potentiation of the anti-metastatic effect of a Ginseng-Salvia miltiorrhiza herbal pair and its biological ingredients via the suppression of CD62E-dependent neutrophil infiltration and NET formation. J Adv Res. 2025;75:739–753. Available from: https://doi.org/10.1016/j.jare.2024.10.036

28. Kim S, Hur SJ, Yang DS. The application of Panax notoginseng with a focus on its anti-inflammatory effect: a narrative review. Ann Transl Med. 2025;13:80. Available from: https://doi.org/10.21037/atm-25-69

29. Sun JM, Liu YX, Tsai YT, Liu YD, Ho CK, Wen DS, et al. Salvianolic acid B protects against UVB-induced HaCaT cell senescence and skin aging through NRF2 activation and ROS scavenging. Photochem Photobiol B. 2025;266:113139. Available from: https://doi.org/10.1016/j.phymed.2024.155676

30. Rehnstam S, Smith SJ, Ahrens L. Suspect and non-target screening of per- and polyfluoroalkyl substances (PFAS) and other halogenated substances in electrochemically oxidized landfill leachate and groundwater. J Hazard Mater. 2024;480:136316. Available from: https://doi.org/10.1016/j.jhazmat.2024.136316

31. Liu Z, Liu F, Wang W, Sun, C, Gao D, Ma J. et al Study of the alleviation effects of a combination of Lactobacillus rhamnosus and inulin on mice with colitis. Food Funct 2020, 11, 3823–3837, https://doi.org/10.1039/c9fo02992c

32. Wirtz S, Popp V, Kindermann M, Gerlach K, Weigmann B, Fichtner-Feigl S.et al . Chemically induced mouse models of acute and chronic intestinal inflammation. Nat Protoc 2017, 12, 1295–1309, https://doi.org/10.1038/nprot.2017.044

33. Yin JZ, Shi XQ, Wang MD, Du H, Zhao XW, Li B. et al Arsenic trioxide elicits anti-tumor activity by inhibiting polarization of M2-like tumor-associated macrophages via Notch signaling pathway in lung adenocarcinoma. Int Immunopharmacol 2023, 117, 109899, https://doi.org/10.1016/j.intimp.2023.109899

34. Zhao R, Zhou Y, Shi H, Ye W, Lyu Y, Wen Z. et al . Effect of Gestational Diabetes on Postpartum Depression-like Behavior in Rats and Its Mechanism. Nutrients 2022, 14, https://doi.org/10.3390/nu14061229

35. Wang H, Chiang C, Xue C, Zhou L, Li S, Zhou Y. et al . Dezocine induces apoptosis in human cervical carcinoma HeLa cells via the endoplasmic reticulum stress pathway. Toxicol Res (Camb) 2022, 11, 498–510, https://doi.org/10.1093/toxres/tfac026

36. Song M, Zhou W, Fan J, Jia C, Xiong W, Wei H. et al Diarrheal microbiota-derived extracellular vesicles drive intestinal homeostasis dysfunction via miR-125b/NF-κB-mediated macrophage polarization. Gut Microbes 2025, 17, 2541036, https://doi.org/10.1080/19490976.2025.2541036

37. Liu XJ, Ye-Er-Tai YL, Jia YB, Wu CH, Wang XX, Yang KM. et al Runchangningshen paste activates NLRP6 inflammasome-mediated autophagy to stimulate colonic mucin-2 secretion and modulates mucosal microbiota in functional constipation. World J Gastroenterol 2025, 31, 102256, https://doi.org/10.3748/wjg.v31.i9.102256

38. Manavi MA, Mohammad Jafari R, Shafaroodi H, Dehpour AR. The Keap1/Nrf2/ARE/HO-1 axis in epilepsy: Crosstalk between oxidative stress and neuroinflammation. Int Immunopharmacol 2025, 153, 114304, https://doi.org/10.1016/j.intimp.2025.114304

39. Lee JWJ, Plichta D, Hogstrom L, Borren NZ, Lau H, Gregory SM. et al Multi-omics reveal microbial determinants impacting responses to biologic therapies in inflammatory bowel disease. Cell Host Microbe 2021, 29, 1294–1304.e1294, https://doi.org/10.1016/j.chom.2021.06.019

40. Fernandes M, Palmieri O, Castellana S, Spanetta M, Latiano T, Lupo C. et al Gut microbiome composition changes in obstructive sleep apnoea syndrome are also in relation to excessive daytime sleepiness. Brain Res Bull 2025, 222, 111251, https://doi.org/10.1016/j.brainresbull.2025.111251

41. Liu H, Yang Z, Chen Q, Zhang H, Liu Y, Wu D. et al The Flavonoid Extract of Polygonum viviparum L. Alleviates Dextran Sulfate Sodium-Induced Ulcerative Colitis by Regulating Intestinal Flora Homeostasis and Uric Acid Levels Through Inhibition of PI3K/AKT/NF-κB/IL-17 Signaling Pathway. Antioxidants (Basel) 2025, 14, https://doi.org/10.3390/antiox14101206

42. Yang S, Fan L, Yin L, Zhao Y, Li W, Zhao R. et Ginseng exosomes modulate M1/M2 polarisation by activating autophagy and target IKK/IκB/NF-κB to alleviate inflammatory bowel disease. J Nanobiotechnology 2025, 23, 198, https://doi.org/10.1186/s12951-025-03292-3

43. Guo Y, Yan H, Zhong C, Gong L, Yang W, Zi Z. et al Quansanqi (derived from Panax notoginseng (Burk.) F. H. Chen) tablets extend the lifespan and ameliorate cellular inflammaging via regulating CD38 and senescence-associated secretory phenotype. J Ethnopharmacol 2026, 357, 120959, https://doi.org/10.1016/j.jep.2025.120959

44. Zhang K, Wang Z, Zhang L, Wu H, Liu J, Zhang M. et al Pharmacologically inherited carbon dots from Salvia miltiorrhiza with potent antioxidant activity and multi-pathway modulation for myocardial ischemia-reperfusion injury therapy. Theranostics 2026, 16, 1855–1876, https://doi.org/10.7150/thno.123141

45. Zhuang W, Qu M, Guan Y, Pan J, Tai Y, Xie G. et al . Houttuynia cordata-derived nanoparticles stabilize mitochondrial dynamics to alleviate ulcerative colitis via the Nrf2/Ho-1 pathways. Phytomedicine 2025, 148, 157505, https://doi.org/10.1016/j.phymed.2025.157505

46. Elshopakey GE, Rezk S, Ateya A, Elkhooly TA, Omar AA, El-Far A. et al Nanoencapsulated Syzygium aromaticum oil alleviates acetic acid-induced ulcerative colitis in rats by influencing critical redox, NF-κB/iNOS, and Keap1/Nrf2/HO-1 signaling pathways. Inflammopharmacology2025, 33, 6719–6752, https://doi.org/10.1007/s10787-025-01939-z

47. Li Y, Wen J, Wu Y, Xu Y, Wu Y, Wang Z. et al Multi-target mechanisms of glabrone in ulcerative colitis: Synergistic restoration of mucosal barrier and inhibition of inflammation through SRC/HSP90 Co-modulation. Biomed Pharmacother 2026, 194, 118951, https://doi.org/10.1016/j.biopha.2025.118951

Citation: Lyu X, Zhang L, Si J, Dai S, Su H, Lyu S, et al. Activation of the Nrf2 Signaling Pathway by a Ginseng-Salvia-Notoginseng Composite Alleviates Ulcerative Colitis via Restoring Gut Microbiota and Intestinal Barrier. Adv Appl of Bioengine. 2026; 2(1): 004-017. Available from: https://dx.doi.org/10.17352/aabe.000003

48. Mondal S, Ganguly A, Nandi A, Das A, Mondal S, Mukherjee S. et al . Network pharmacology and molecular docking reveal multi-target mechanisms of Butea monosperma stem bark extract in ulcerative colitis. Sci Rep 2025, 15, 40302, 24091-8. https://doi.org/10.1038/s41598-025-24091-8

49. hang Z, Zhou L, Liu Y, Yang X, Yao D, Zhai F, Liu B, et al. Tongxie Yaofang attenuates ulcerative colitis by modulating gut microbiota and IL-10RA/NF-κB-mediated macrophage polarization. Phytomedicine 2025, 148, 157459, doi:10.1016/j.phymed.2025.157459.

50. He G, Sun J, Gu Y, Zheng Y, Wang L, Sun Y. Network analysis and in vivo experiments reveal the therapeutic mechanisms of total ginsenosides in a Drosophila model of ulcerative colitis. Front Pharmacol 2025, 16, 1556579, https://doi.org/10.3389/fphar.2025.1556579

51. Li W, Shi H, Wu X. A narrative review of Panax notoginseng: Unique saponins and their pharmacological activities. J Ginseng Res 2025, 49, 118–133, https://doi.org/10.1016/j.jgr.2024.12.005

52. Yang K, Liu YJ, Zhang JN, Chen YJ, Yang J, Xiao JP. et al Advances in the structural characterization and pharmacological activity of Salvia miltiorrhiza polysaccharides. Front Chem 2025, 13, 1492533, https://doi.org/10.3389/fchem.2025.1492533

53. Ma QS, Chen QL, Wu GP, Yao YW, Fan YX, Linghu KG. et al . Sigesbeckia pubescens makino alleviates ulcerative colitis in mice by modulating the Nrf2/Keap1 pathway. Front Pharmacol 2025, 16, 1588525, https://doi.org/10.3389/fphar.2025.1588525

54. Li G, Liu R, Peng Z, Zhang S, Sun R, Wang Z. et al . Inhibition of CAV1 attenuates diabetic cardiomyopathy by reducing ferroptosis via activating the NRF2/GCLC signaling pathway. Theranostics 2025, 15, 4989–5006, https://doi.org/10.7150/thno.107367

55. Wang H, Yang Y, Ye Y, Wei X, Chen S, Cheng B. et al . Srxn1 Overexpression Protects Against Cardiac Remodelling by Inhibiting Oxidative Stress and Inflammation. J Cell Mol Med 2025, 29, e70432, https://doi.org/10.1111/jcmm.70432

56. Bagheri GR, Poursamimi J, Ali-Anvari H, Rashki Ghalenoo S, Ghaffari HR. The Immune Base Therapy of Pain with Magnesium Sulfate on the Trigger Axis of the TNF-α-TRAF6-NF-κB and Its Inhibitor (miR-146a-5p) in Rats. Iran J Allergy Asthma Immunol 2025, 24, 180–186,

57. Ou H, Huang H, Xu Y, Lin H, Wang X. Systematic druggable genome-wide Mendelian randomization to identify therapeutic targets and dominant flora for ulcerative colitis. Pharmacol Res 2025, 213, 107662, https://doi.org/10.18502/ijaai.v24i2.18146

58. Shi JY, Wang YJ, Bao QW, Qin YM, Li PP, Wu QQ. et al Polygonatum cyrtonema Hua polysaccharide alleviates ulcerative colitis via gut microbiota-independent modulation of inflammatory immune response. Carbohydr Polym 2025, 356, 123387, https://doi.org/10.1016/j.carbpol.2025.123387

59. Deng B, Wang K, He H, Xu M, Li J, He P. et . Biochanin A mitigates colitis by inhibiting ferroptosis-mediated intestinal barrier dysfunction, oxidative stress, and inflammation via the JAK2/STAT3 signaling pathway. Phytomedicine 2025, 141, 156699, https://doi.org/10.1016/j.phymed.2025.156699

60. Cao L, Tang X, Wang X, Wang Y, Dai W. Psoralen alleviates ulcerative colitis by suppressing inflammation, modulating oxidative stress, and regulating ferroptosis. Eur J Pharmacol 2025, 1005, 178081, https://doi.org/10.1016/j.ejphar.2025.178081

61. Fu W, Huang Z, Li W, Xu L, Yang M, Ma Y. et al Copper-luteolin nanocomplexes for mediating multifaceted regulation of oxidative stress, intestinal barrier, and gut microbiota in inflammatory bowel disease. Bioact Mater 2025, 46, 118–133, https://doi.org/10.1016/j.bioactmat.2024.12.004

62. Rubin DT, Ananthakrishnan AN, Siegel CA, Barnes EL, Long MD. ACG Clinical Guideline Update: Ulcerative Colitis in Adults. Am J Gastroenterol 2025, 120, 1187–1224, https://doi.org/10.14309/ajg.0000000000003463

63. Gefen R, Dourado J, Emile SH, Wignakumar A, Rogers P, Aeschbacher P. et al Fecal microbiota transplantation for patients with ulcerative colitis: a systematic review and meta-analysis of randomized controlled trials. Tech Coloproctol 2025, 29, 103, https://doi.org/10.1007/s10151-025-03113-7

64. Ge C, Lu Y, Shen Z, Lu Y, Liu X, Zhang M. et al Machine learning and metabolomics identify biomarkers associated with the disease extent of ulcerative colitis. J Crohns Colitis 2025, 19, https://doi.org/10.1093/ecco-jcc/jjaf020

Citation: Lyu X, Zhang L, Si J, Dai S, Su H, Lyu S, et al. Activation of the Nrf2 Signaling Pathway by a Ginseng-Salvia-Notoginseng Composite Alleviates Ulcerative Colitis via Restoring Gut Microbiota and Intestinal Barrier. Adv Appl of Bioengine. 2026; 2(1): 004-017. Available from: https://dx.doi.org/10.17352/aabe.000003